A comparison between double-PFG MRI and DTI in *ex vivo* rat brain

Tuukka Miettinen[1], Alejandra Sierra[1], Teemu Laitinen[1], Juhana Sorvari[1], and Olli Gröhn[1]
[1]*Department of Neurobiology, A. I. Virtanen Institute, University of Eastern Finland, Kuopio, Kuopio, Finland*

Introduction

Diffusion Tensor Imaging (DTI) is an established non-invasive imaging method to study coherently oriented structures, present mainly in the white matter in brain. However, the information obtained by DTI is limited when tissue microstructures are randomly oriented within an imaging voxel, as is often the case in the grey matter. Recently, it has been suggested that angular double-pulsed-field-gradient (d-PFG)[1, 2, 3] techniques may provide MRI contrasts also, when the tissue consists of randomly oriented anisotropic structures[2]. In this approach, two diffusion gradient pairs are applied offering many degrees of freedom, and the diffusion periods, mixing time and the angle between the gradient pairs can be varied. The aim of this study was to compare the contrast generated by DTI and angular d-PFG in different brain regions with different degrees of macroscopic and microscopic anisotropy as verified by histology.

Methods

Adult Sprague Dawley rats (n=6) were perfused using 4% paraformaldehyde-1% glutaraldehyde, and brains were immersed in perfluoropolyethylen (Galden) for *ex vivo* imaging. All MRI experiments were performed in a vertical 9.4 T magnet interfaced to a Varian DirectDrive console using a quadrature volume RF-coil. Data were acquired using a double-pulsed gradient spin echo (d-PGSE) -sequence (TR = 3 s and TE = 60 ms). The following d-PGSE imaging parameters were used: t_m = 2 ms, $\delta_1 = \delta_2$ = 4 ms, $\Delta_1 = \Delta_2$ = 20 ms and $|G_1| = |G_2|$ = 230 mT/m. The FOV of 18 x 18 mm^2 was covered with a 128 x 128 points resulting in spatial resolution of 140 x 140 µm^2. Fifteen slices with slice thickness of 750 µm covered the entire cerebrum. The angular d-PFG experiment was performed in X-Y plane (=axial plane) with twelve 30° steps (ψ-values) and 8 average resulting in 11 hours of scan time. Data were normalized ($E(\psi)_{norm} = E(\psi)/(E(\psi=0°) + E(\psi=360°))$) and the d-PFG maps calculated by fitting data into the following equation: $E(\Psi)_{norm} = 1 - aE * [\sin^2(\psi + \varphi)] + C$ in which aE = apparent eccentricity and φ = residual phase[2]. For comparison, DTI data were acquired using the same spin echo pulse sequence and parameters except diffusion weighting in six directions with b-value of 1000 s/mm^2, 8 averages, total scan time of 6 hours. FA and DEC maps were calculated from DTI data using the dtifit program provided by FSL. After MRI, brains were processed for histology and selected sections were stained with gold chloride staining (myelinated-axons) or Nissl staining (cytoarchitecture, data not shown)

Results

Fig. 1 shows fractional anisotropy (FA) and direction encoded color (DEC) maps (Fig. 1A and 1C) calculated from DTI data and apparent eccentricity (aE) and residual phase (φ) (Fig. 1B and 1D) calculated from d-PFG data. We selected five representative regions of interest (ROI) based on their different cytoarchitecture and myeloarchitecture: two in white matter (corpus callosum (cc) and internal capsule (ic)) and three in grey matter (ventrobasal complex (VB), dentate gyrus (DG) and primary somatosensory cortex (S1)) (Fig. 1A and 3A). In white matter areas, both cc and ic presented similar very high FA values (>0.8) (Fig. 2A). In contrast |aE| of cc (0.47 ± 0.08) was four times higher than |aE| of ic (0.13 ± 0.03) (Fig. 2B). In histology, the cc showed coherently oriented myelinated bundles of axons running in parallel (Fig. 3B), while in the ic significant amount of the crossing axon bundles are present (Fig. 3C). This is reflected also in the residual phase difference, where cc had a positive residual phase shift (0.26 ± 0.08) and the ic had a very low residual phase shift (-0.03 ± 0.14) (Fig. 2C). In gray matter areas, FA values were lower than in white matter (Fig. 2A), along with lower |aE| values (Fig. 2B). The composition in these areas was a mixture of coherently oriented myelinated axons (Fig. 3D-F), and more randomly oriented cell bodies and processes (data not shown). These areas showed different amounts of residual phase (Fig. 2C) that could be attributed to different degrees of coherence in myelinated axons (Fig. 3D-F).

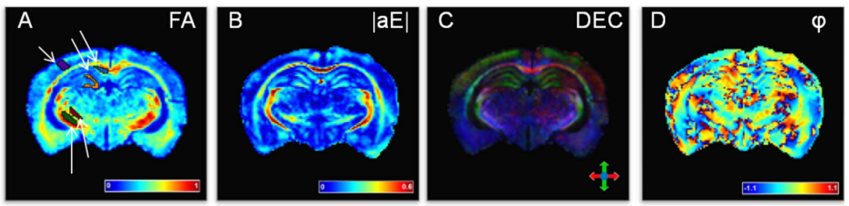

Fig 1. (**A**) A Fractional anisotropy (FA) map, (**B**) an absolute value of apparent eccentricity (|aE|) map, (**C**) a direction-encoded color (DEC) FA-map, (**D**) a residual phase map (φ) from one representative slice in the level of dorsal hippocampus.

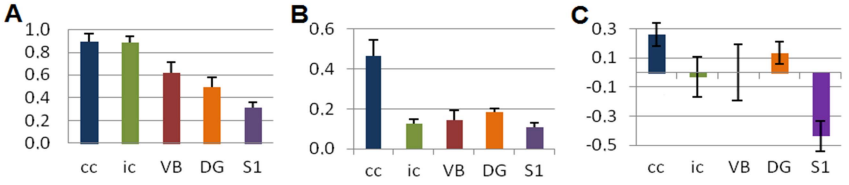

Fig 2. Quantification of the calculated parameters (mean value and standard deviation) from five regions of interest (white arrows in Fig **1A**). (**A**) A fractional anisotropy (FA), (**B**) an absolute-valued apparent eccentricity (aE) and (**C**) a residual phase (φ).

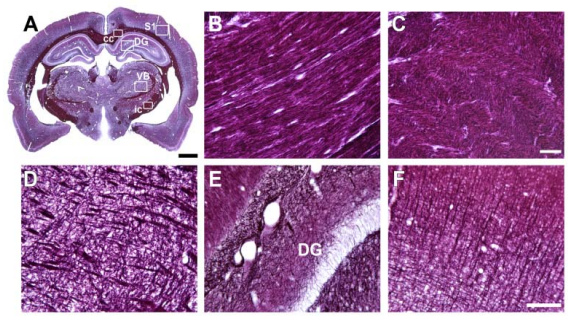

Fig 3. (**A**) Photomicrograph of a myelin stained section. White squares indicate the selected areas shown in higher magnification photomicrographs panels B-F, (**B**) corpus callosum (cc), (**C**) internal capsule (ic), (**D**) ventrobasal complex (VB), (**E**) dentate gyrus (DG) and (**F**) primary somatosensory cortex (S1). Scale bars: 1mm (**A**), 50 µm (**B**, **C**) and 150 µm (**D**, **E**, **F**).

Discussion and Conclusion

It has been suggested that angular d-PFG MRI provides new indices of microstructural features of tissue. Our *ex vivo* d-PFG/DTI data show clear differences between parametric maps obtained from DTI and d-PFG from different kind of microstructural organization as assessed by histology. The major differences were shown between FA and |aE| in white matter while the residual phase map offers improved contrast in grey matter. We conclude that double-PFG can provide novel information about microstructure of tissue both in white and grey matter structure and it has potential to detect structural modifications caused by different kind of pathological conditions.

References

[1]Shemesh N, et al. NMR Biomed. 2010; 23:757-780. [2]Shemesh N, et al. Magnetic Resonance in Medicine. 2012; 68:794-806. [3]Mitra PP, Phys. Rev. B. 1995; 51:15074.